View metadata, citation and similar papers at core.ac.uk
brought to you by CORE
provided by E-resource repository of the University of Latvia

# Effect of Ga content on luminescence and defects formation processes in $Gd_3(Ga,Al)_5O_{12}$:Ce single crystals

L. Grigorjeva [a], K. Kamada [b], M. Nikl [c], A. Yoshikawa [d], S. Zazubovich [e, *], A. Zolotarjovs [a]

[a] Institute of Solid State Physics, University of Latvia, Kengaraga 8, Riga, LV-1063, Latvia
[b] New Industry Creation Hatchery Center, Tohoku University, 2-1-1 Katahira, Aoba-ku, Sendai, 980-8577, Japan
[c] Institute of Physics AS CR, Cukrovarnicka 10, 16253, Prague 6, Czech Republic
[d] Institute for Materials Research, Tohoku University, 2-1-1, Katahira, Aoba-ku, Sendai, Miyagi, 980-8577, Japan
[e] Institute of Physics, University of Tartu, W. Oswaldi 1, 50411, Tartu, Estonia

a b s t r a c t

Luminescence characteristics of $Ce^{3þ}$ - doped $Gd_3Ga_xAl_{5-x}O_{12}$ single crystals with different Ga contents (x ¼ 1, 2, 3, 4, 5) are studied in the 9e500 K temperature range. The spectra of the afterglow, photo-luminescence, radioluminescence, and thermally stimulated luminescence (TSL) of each crystal coincide. The increase of the Ga content results in the high-energy shift of the spectra while the radioluminescence intensity at 9 K remains practically constant up to x ¼ 4. No $Ce^{3þ}$ emission is observed in case of x ¼ 5. The total TSL intensity drastically increases, reaches the maximum value around x ¼ 2e3, and then decreases due to the thermal quenching of the $Ce^{3þ}$ emission. The TSL glow curve maxima are gradually shifting to lower temperatures, and the dependence of the maxima positions and the corresponding trap depths on the Ga content is close to linear. However, the activation energy of the TSL peaks creation under irradiation of the crystals in the 4f e $5d_1$ absorption band of $Ce^{3þ}$ decreases drastically with the increasing Ga content (especially in the range of x ¼ 1e2), and this dependence is found to be strongly nonlinear. Possible reasons of the nonlinearity are discussed.

## 1. Introduction

In recent years, the Ce - doped $Gd_3Ga_xAl_{5-x}O_{12}$ single crystals, ceramics and epitaxial films with different Ga contents (x) were intensively studied as promising scintillator materials for their application in medical imaging because of their extremely high light yield, good energy resolution, relatively high density (6.63 g/ $cm^3$), fast scintillation response, and high radiation stability and hardness [1e25]. Single crystals of $Gd_3Ga_xAl_{5-x}O_{12}$:Ce prepared by the micro-pulling down method were first reported in Ref. [1]. Their scintillation characteristics were found to depend on the Ga concentration. For the crystal with x ¼ 3, the light yield of z42 000 photons/MeV, the dominating decay time of z53 ns, and the en-ergy resolution of 8.3%@662 keV were obtained. With the decreasing Ga content, the light yield and energy resolution were found to improve, but the decay time increases. The first $Gd_3Ga_3Al_2O_{12}$:Ce single crystal grown by the Czochralski method with the light yield of 46 000 photons/MeV and energy resolution of 4.9%@662 keV was reported in Ref. [2]. Recently, an extremely high light yield of 58 000 photons/MeV and the best energy reso-lution of 4.2%@662 keV were obtained for the single crystals of $Gd_3Ga_xAl_{5-x}O_{12}$:Ce with x ¼ 2.7 and x ¼ 2.4, respectively, also grown by the Czochralski method [11]. Due to these characteristics, $Gd_3Ga_xAl_{5-x}O_{12}$:Ce with x ¼ 2e3 was considered as a promising scintillator for the PET application [2].

The systematic photoluminescence study of $Gd_3Ga_xAl_{5-x}O_{12}$:Ce showed that the increasing Ga content results in the high-energy shift of the $Ce^{3þ}$ - related $5d_1$ e 4f emission band and the lowest-energy 4f e $5d_1$ absorption (excitation) band as well as in the low-energy shift of the 4f e $5d_2$ excitation band [6,24]. The Stokes shift slightly increases as well. The decrease of both the crystal field strength and the band gap of the host material was reported (see, e.g. [4,6], and references therein). According to [6], the activation energy of thermal quenching of the $5d_1$ e 4f emission determined from the temperature dependence of the luminescence decay time decreases linearly from $E_q$ z 0.6 eV for x ¼ 0 to $E_q$ z 0.07 eV for x ¼ 4. The TSL characteristics were studied for $Gd_3Ga_3Al_2O_{12}$:Ce crystals in Refs. [9,10,13], for the $Gd_3Ga_xAl_{5-x}O_{12}$:Ce epitaxial films

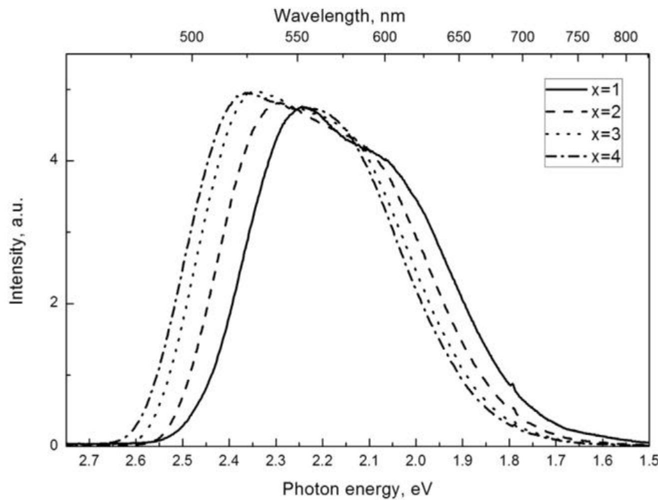


Fig. 1. X-ray excited luminescence spectra of the $Gd_3Ga_xAl_{5-x}O_{12}$:Ce single crystals with different Ga contents (shown in the legend) measured at the same conditions at T¼9K.

with the Ga content varying from x ¼ 2.7 to x ¼ 3.54, in Ref. [23], and for the $Gd_3Ga_xAl_{5-x}O_{12}$:Ce single crystal with x ¼ 2.83, in Ref. [25], i.e., the x values in the previous studies varied only from 2.7 to 3.54.

In the present work, the characteristics of the photo- and X-ray excited luminescence and TSL of the $Gd_3Ga_xAl_{5-x}O_{12}$:Ce single crystals with different Ga contents (x ¼ 1, 2, 3, 4, 5) grown by the micro-pulling down method are measured in a wide temperature range (9e500 K) and compared. The aim of this work is to inves-tigate the dependences of these characteristics on the Ga content, to explain the mechanisms of these dependences, and to clarify a possible role of $Ga^{3þ}$ ions in the defects formation processes in these scintillation materials.

## 2. Experimental procedure

Single crystals of $Gd_3Ga_xAl_{5-x}O_{12}$:Ce with the same (0.2 at.%) Ce content and different Ga contents (x ¼ 1, 2, 3, 4, 5) were grown by the micro-pulling down method [1]. Pieces of the grown crystals were crushed and ground into a powder in a mortar. Powder X-ray diffraction (XRD) analysis was carried out in the 2q range 15 e75 using a RINT Ultima (RIGAKU) diffractometer. Cu Ka X-ray source was used, and the accelerating voltage and current were 40 kV and 40 mA, respectively. Quantitative chemical analysis of the crystals for Al, Ce, Y and Gd content along the growth direction was per-formed by electron probe microanalysis (EPMA; JXA-8621MX, JEOL), for the details see Ref. [1]. Disks of about 1 mm thickness were cut from crystal rods of about 3 mm diameter and polished up to a optical grade.

The steady-state emission and excitation spectra in the 85e500 K temperature range were measured using a setup, con-sisting of the LOT - ORIEL xenon lamp (150 W), two mono-chromators (SF - 4 and SPM - 1) and nitrogen cryostat. The luminescence was detected by a photomultiplier (FEU - 39 or FEU - 79) connected with an amplifier and recorder.

The X-ray excited luminescence and afterglow spectra were measured at 9 K after a crystal was irradiated with the X-ray tube (40 kV, 15 mA) for 10 min to achieve the intensity saturation. The luminescence was detected using Andor Shamrock B-303i spec-trograph coupled to Andor DU-401A-BV CCD camera.

TSL glow curves $I_{TSL}(T)$ were measured with a heating rate of 0.2 K/s at two different setups. At the first setup, the TSL glow curves were measured in the 85e500 K temperature range after selective ultraviolet (UV) irradiation of the crystals at different temperatures $T_{irr}$ with different irradiation photon energies $E_{irr}$. A crystal located in a nitrogen cryostat was irradiated with the LOT - ORIEL xenon lamp (150 W) through a monochromator SF - 4. The spectral width of the monochromator slit did not exceed 5 nm. The TSL glow curves were measured with the monochromator SPM - 1 and detected with the photomultiplier FEU - 39 and recorder. For each TSL glow curve peak, the TSL peak creation spectrum, i.e., the dependence of the maximum TSL intensity ($I^{max}_{TSL}$) on the irradiation photon energy $E_{irr}$, was measured. From the dependence of the maximum TSL intensity ($I^{max}_{TSL}$) on the irradiation temperature $T_{irr}$, the activation energy $E_a$ for the TSL peak creation was determined. To determine the trap depth $E_t$ corresponding to each TSL peak, the partial cleaning method was used (for more details, see, e.g. [26], and references therein). The crystal, irradiated at the temperature $T_{irr}$, was cooled down to 85 K, heated up to a temperature $T_{stop}$, then quickly cooled down to 85 K and the TSL glow curve was recorded. In the next cycle, the same procedure was repeated for the different temperature $T_{stop}$, etc. From the slope of the $ln(I_{TSL})$ as a function of the reverse temperature (1/T), the $E_t$ value was calculated.

At the second setup, the TSL spectra and glow curves were measured in the 9e300 K temperature range after X-ray irradiation of the crystals with the X-ray tube (40 kV, 15 mA) for 5 min. The luminescence was detected using Andor Shamrock B-303i spec-trograph coupled to Andor DU-40 1A-BV CCD camera. Trap depths were determined using fractional glow technique [27].

## 3. Experimental results and discussion

The radioluminescence spectra of $Gd_3Ga_xAl_{5-x}O_{12}$:Ce measured at the same conditions at 9 K are shown in Fig. 1. The position of the center of the doublet $Ce^{3þ}$ - related emission band ($E_{em}$) and its full width at half maximum (FWHM) for each crystal are presented in Table 1. It is evident that the emission band is shifting to high en-ergies with the increasing Ga content while the radioluminescence intensity at 9 K remains practically constant up to x ¼ 4. No $Ce^{3þ}$ emission is observed in case of x ¼ 5. The photoluminescence spectra as well as the spectra of the afterglow and low-temperature TSL of each sample coincide with the spectra shown in Fig. 1. The photoluminescence excitation spectrum consists of several bands

Table 1
The position ($E_{em}$) and FWHM of the X-ray excited luminescence band at 9 K, activation energy $E_q$ of the luminescence thermal quenching obtained in the present work from the I(T) dependences measured in the T > 430 K temperature region and in Ref. [6] from the temperature dependences of the decay times, activation energy $E_a$ of the TSL peaks creation under irradiation in the 4f e $5d_1$ absorption band of $Ce^{3þ}$, and the energy difference $E_{dc}$ between the $5d_1$ level of $Ce^{3þ}$ and the bottom of the CB estimated in this work and reported in Ref. [29] for the $Gd_3(Ga,Al)_5O_{12}$:Ce single crystals with different Ga contents.

| Crystal | $E_{em}$, eV | FWHM, eV | $E_q$, eV | $E_q$, eV [6] | $E_a$, eV | $E_{dc}$, eV | $E_{dc}$, eV [29] |
|---|---|---|---|---|---|---|---|
| $Gd_3Ga_1Al_4O_{12}$:Ce | 2.15 | 0.46 | 0.40 | 0.43 | 1.04 | 1.04 | 0.56 |
| $Gd_3Ga_2Al_3O_{12}$:Ce | 2.20 | 0.47 | 0.42 | 0.49 | 0.32 | 0.76 | 0.52 |
| $Gd_3Ga_3Al_2O_{12}$:Ce | 2.23 | 0.49 | 0.33 | 0.27 | 0.16 | 0.50 | 0.36 |
| $Gd_3Ga_4Al_1O_{12}$:Ce | 2.25 | 0.50 | 0.34 | 0.07 | 0.08 | 0.25 | 0.18 |

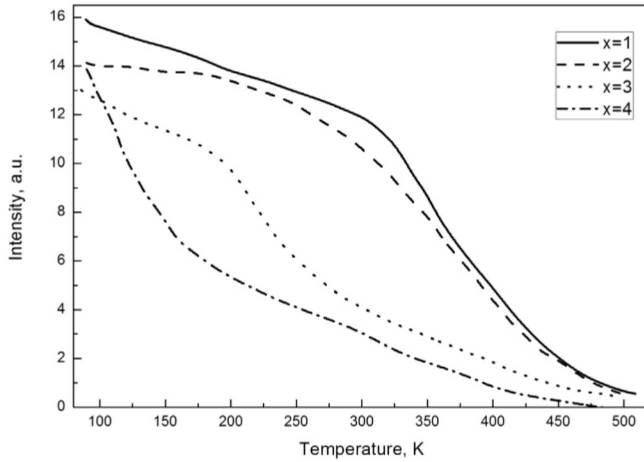


Fig. 2. Temperature dependences of the maximum $Ce^{3þ}$ - related luminescence in-tensity measured under excitation in the maximum of the 4f e $5d_1$ absorption band of $Ce^{3þ}$ centers.

arising from the 4f e 5d transitions of $Ce^{3þ}$ ions. The dependences of the emission and excitation spectra of the investigated $Gd_3Ga_xAl_{5-x}O_{12}$:Ce crystals on the Ga content are similar to those reported earlier and explained by the shrinkage of the forbidden gap and changes in the energies of the $5d_1$, $5d_2$ excited states of $Ce^{3þ}$ with respect to the 4f ground state of $Ce^{3þ}$ and the bottom of the conduction band (CB) (see, e.g. [4,6,24], and references therein). Temperature dependences of the $Ce^{3þ}$ - related photoluminescence intensity (Fig. 2) indicate that the activation energy $E_q$ of the luminescence thermal quenching strongly decreases with the increasing Ga content (see also [6,24]). At the temperature dependence of the $5d_1$ e 4f luminescence intensity (I) demon-strated for some crystals in the lnI e 1/T coordinates (Fig. 3), several stages with different activation energies $E_q$ can be observed. The $E_q$ values obtained in the high-temperature range (430e500 K) are shown in Table 1.

After X-ray irradiation of the crystals at 9 K as well as after their UV irradiation at an appropriate temperature in the maximum of the 4f - $5d_2$ (around 3.6 eV) or 4f e $5d_1$ (around 2.8 eV) absorption band of $Ce^{3þ}$, the $Ce^{3þ}$ - related TSL appears due to the creation of the recombining electron centers and the hole $Ce^{4þ}$ centers. The TSL glow curves measured for the $Gd_3Ga_xAl_{5-x}O_{12}$:Ce single crystals

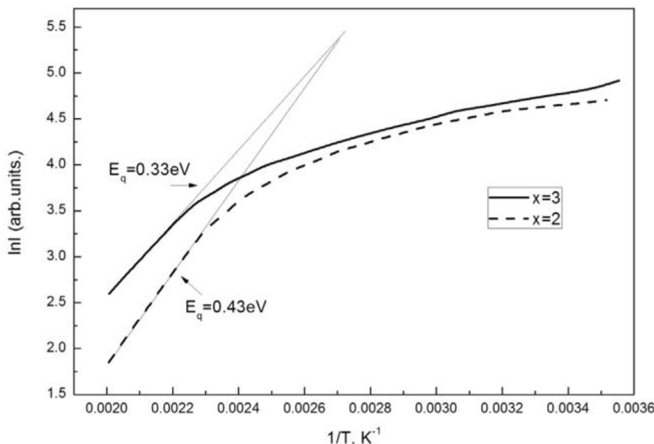


Fig. 3. Some selected temperature dependences of the $5d_1$ e 4f luminescence intensity (I) presented the ln I e 1/T coordinates and the activation energies $E_q$ of the lumi-nescence thermal quenching in the high-temperature range.

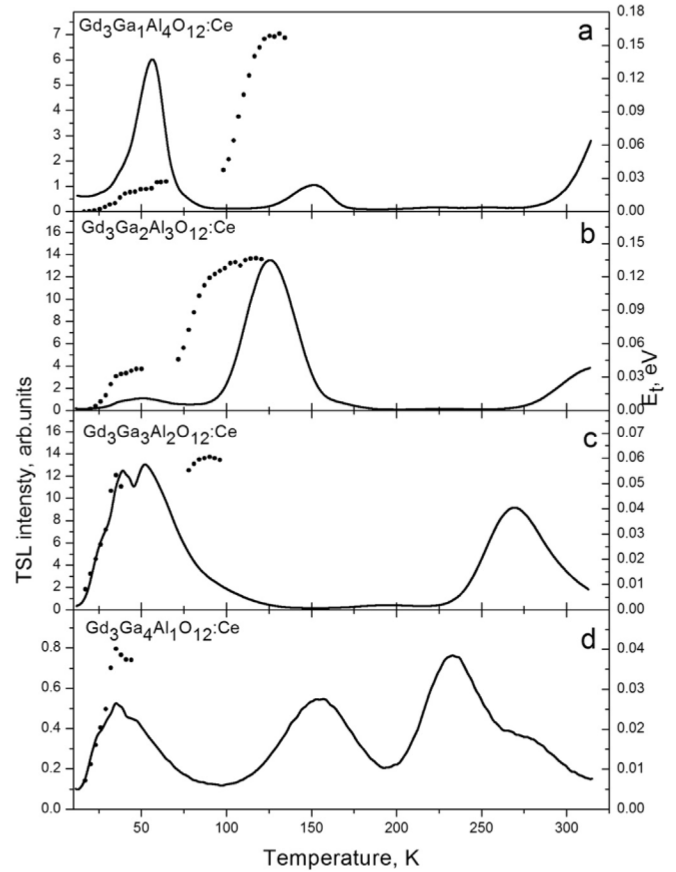


Fig. 4. TSL glow curves measured for the $Gd_3Ga_xAl_{5-x}O_{12}$:Ce single crystals with different Ga contents after their X-ray irradiation at 9 K (solid lines) and the trap depths $E_t$ corresponding to the lowest-temperature TSL peaks (filled circles).

with different Ga contents are shown in Figs. 4 and 5. For the $Gd_3Ga_3Al_2O_{12}$:Ce crystal (Figs. 4c and 5c), the TSL glow curve is similar to those obtained in Refs. [9,10,13,25] for analogous crystals grown using the Czochralski technique, however, the intensity ra-tios of the low-temperature and the high-temperature TSL peaks are strongly different. The TSL peak positions are presented in Table 2. All the TSL glow curve peaks are complex and consist of several components (see also [9,10,13]). This is evident from the comparison of the TSL glow curves measured after the UV irradi-ation at different temperatures $T_{irr}$ and appears also in the exper-iments with partial heating. The total TSL intensity increases (z50 times) with the increasing Ga content and reaches the maximum around x ¼ 2 and x ¼ 3, indicating strongly increasing concentra-tion of electron traps in these crystals. In the sample with x ¼ 4, the total TSL intensity decreases by about an order of magnitude due to the thermal quenching of the $Ce^{3þ}$ emission (Fig. 2). Due to the same reason, the intensity ratio of the low-temperature and high-temperature TSL peaks presented in Figs. 4 and 5 is also per-turbed. No $Ce^{3þ}$ - related TSL is observed in the sample with x ¼ 5.

From the TSL data, the parameters of the traps (trap depths $E_t$ and frequency factors $f_0$) corresponding to each TSL can be deter-mined (Table 2). The dependences of the trap depth $E_t$ on the temperature $T_{stop}$ are presented in Figs. 4 and 5 (filled circles). The presence of the $E_t(T_{stop})$ dependence in the range of a TSL peak is an evidence of its complex structure (see also [10,13]). The positions of the peaks at the TSL glow curve obtained after X-ray irradiation of the crystals at 9 K are found to be independent of the irradiation duration (measured up to $t_{irr}$ ¼ 2 h). This confirms the first-order

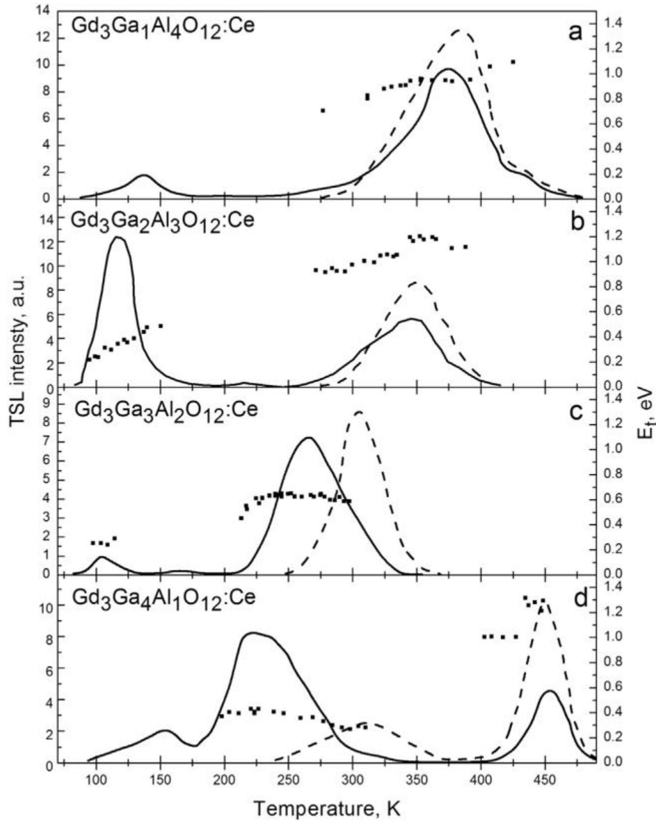


Fig. 5. TSL glow curves measured for the $Gd_3Ga_xAl_{5-x}O_{12}$:Ce single crystals with different Ga contents after their UV irradiation at 85 K in the 4f e $5d_2$ absorption band of $Ce^{3þ}$ (solid line) and after irradiation at 295 K in the 4f e $5d_1$ absorption band of $Ce^{3þ}$ (dashed line) and the corresponding trap depths $E_t$ (filled circles).

Table 2
The TSL peaks positions ($T_m$), trap depths ($E_t$), and frequency factors ($f_0$) obtained for the $Gd_3(Ga,Al)_5O_{12}$:Ce single crystals with different Ga contents.

| Crystal | $T_m$, K | $E_t$, eV | $f_0$, s 1 |
|---|---|---|---|
| $Gd_3Ga_1Al_4O_{12}$:Ce | 56 | 0.03 | $10^1$ |
| | 138 | e | e |
| | 375 | 0.90e0.95 | $10^{10}$ |
| $Gd_3Ga_2Al_3O_{12}$:Ce | 50 | 0.04 | $10^2$ |
| | 118 | 0.14e0.24 | $10^7$e$10^9$ |
| | 342 | 0.78e0.86 | $10^{10}$ |
| $Gd_3Ga_3Al_2O_{12}$:Ce | 46 | 0.05 | $10^4$ |
| | 105 | 0.25 | $10^{10}$ |
| | 268 | 0.60e0.64 | $10^{10}$ |
| $Gd_3Ga_4Al_1O_{12}$:Ce | 34 | 0.04 | $10^5$ |
| | 152 | e | e |
| | 232 | 0.38e0.42 | $10^8$ |
| | 450 | 1.0 | $10^9$ |

recombination kinetics reported for $Gd_3Ga_3Al_2O_{12}$:Ce in Refs. [9,10,13]. In this case, the frequency factors $f_0$ can be calculated using the expression

$$f_0 ¼ (bE_t / kT^2_m) \exp (E_t / kT_m)$$

where b is the crystal heating rate, k is the Boltzmann factor, and $T_m$ is the maximum position of the considered TSL peak. Due to a complex structure of the TSL peaks, only approximate values of the $E_t$ and $f_0$ parameters could be obtained. The $T_m$ value is taken as the temperature where the peak position becomes independent of $T_{stop}$. According to our estimations, $T_m$ values for the main TSL peaks can be defined with an accuracy of about 2e5 K. The values of $E_t$ are defined with an accuracy of about 5e10%. For the $f_0$ values, only an order of magnitude can be roughly estimated.

In Fig. 6, the dependences of the higher-temperature TSL peak position (filled triangles) and the corresponding trap depth value $E_t$ (empty circles) on the Ga content are presented. These de-pendences can be explained by the $Ga^{3þ}$ - induced lowering of the CB bottom energy with the increasing Ga content (see, e.g., [4,28]). Both these dependences are found to be close to linear. Similar dependences have been also obtained for some other $Ce^{3þ}$ - doped multicomponent garnets (see, e.g. [23,28], and references therein).

The dependences of the TSL peak intensity on the irradiation duration $t_{irr}$ are found to depend on the TSL peak and the crystal irradiation temperature and energy. Some selected dose de-pendences measured for the $Gd_3Ga_3Al_2O_{12}$:Ce crystal are shown in Fig. 7. A quick saturation of the TSL intensity (curves 1 and 2), probably caused by a close location of the recombining electron and hole centers, is observed also for the 160 K peak in the crystal with x ¼ 4 irradiated at 85 K in the 4f e $5d_2$ absorption band of $Ce^{3þ}$. The dependence similar to curve 3 in Fig. 7 is observed for the TSL peaks at 342 K and 375 K in the crystals with x ¼ 2 and x ¼ 1, respectively, irradiated at 85 K in the 4f e $5d_2$ absorption band of $Ce^{3þ}$.

From the dependence of the TSL peak intensity on the irradia-tion temperature $T_{irr}$ presented in the ln($I_{TSL}$) e 1/$T_{irr}$ coordinates (Fig. 8), the activation energy $E_a$ can be determined for the TSL peaks creation (Table 1). The data obtained indicate that in the crystal with x ¼ 1, the $5d_2$ level is located slightly below the con-duction band and $E_a$ z 0.07 eV. Taking into account the $5d_1$ e $5d_2$ energy distance (0.97 eV) which can be obtained from the excita-tion spectrum of the $Ce^{3þ}$ emission in this crystal, the activation energy for the TSL peaks creation under irradiation in the 4f e $5d_1$ absorption band of $Ce^{3þ}$ is estimated to be $E_a$ z 1.04 eV. For the crystals with a higher Ga content, the $5d_2$ level is located inside the conduction band.

Usually, the $Ce^{3þ}$ luminescence thermal quenching and the appearance of TSL peaks are both explained as a result of the photostimulated electron release from the lowest-energy excited $5d_1$ level of $Ce^{3þ}$ into the CB. If this is the case, the values of the activation energies $E_q$ and $E_a$ should be close and correspond to the energy distance between the $5d_1$ excited level of $Ce^{3þ}$ and the

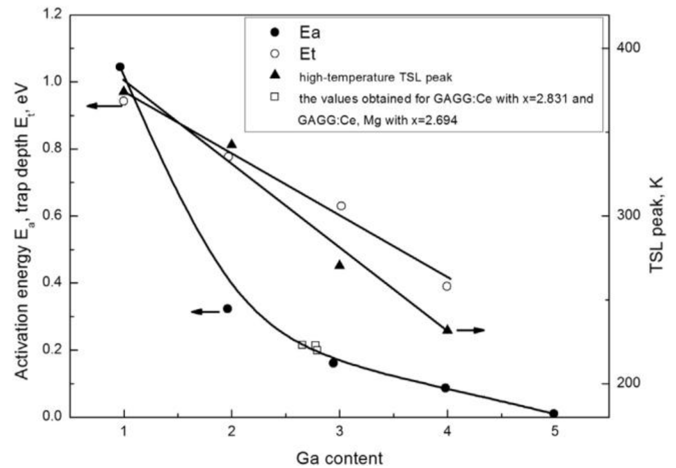


Fig. 6. Dependences of the activation energy $E_a$ of the TSL peaks creation (filled cir-cles), the position of the high-temperature TSL peak (filled triangles), and the corre-sponding trap depth $E_t$ (empty circles) on the Ga content obtained for the $Gd_3Ga_xAl_{5-x}O_{12}$:Ce single crystals. The $E_a$ values obtained in Ref. [25] for the Ce - doped crystal with x ¼ 2.831 and for the Ce, Mg co - doped crystal with x ¼ 2.694 are shown by empty squares.

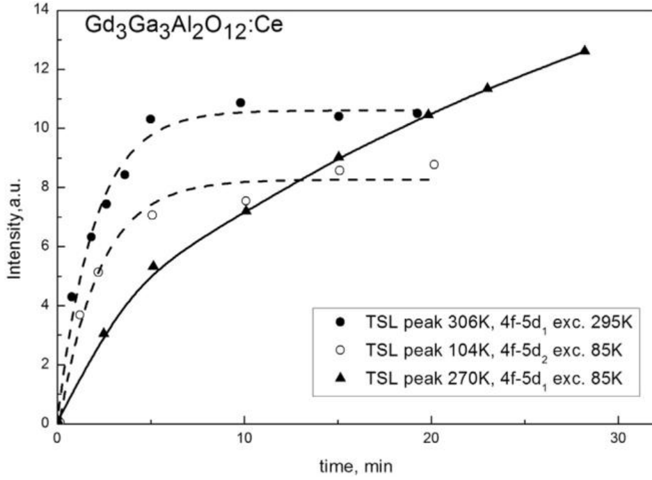


Fig. 7. Dependences of the TSL intensity on the irradiation duration $t_{irr}$ measured for the $Gd_3Ga_3Al_2O_{12}$:Ce single crystal. The selected TSL peaks and irradiation conditions are shown in the legend.

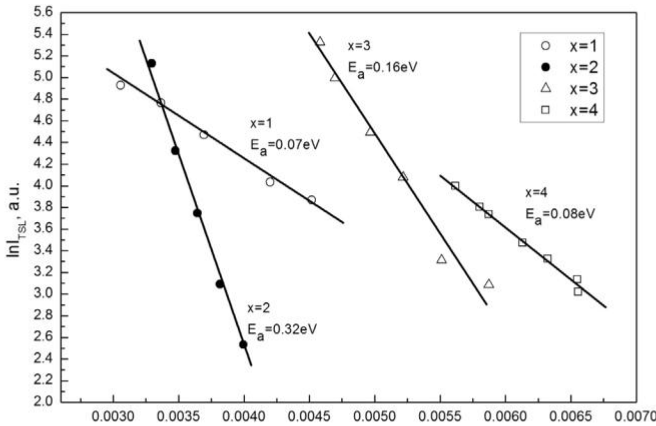


Fig. 8. Dependences of the TSL intensity ($I_{TSL}$) on the irradiation temperature ($T_{irr}$) presented in the ln($I_{TSL}$) e $1/T_{irr}$ coordinates and the values of the corresponding activation energies $E_a$ obtained for different $Gd_3Ga_xAl_{5-x}O_{12}$:Ce single crystals.

bottom of the CB. However, the $E_a$ values differ from the activation energies $E_q$ of the $5d_1$ e 4f emission thermal quenching determined both in the present work from the temperature dependences of the maximum emission intensity (see, e.g., Fig. 3) and in Ref. [6], from the temperature dependence of the luminescence decay time (Table 1). It should be noted that the stage with the activation en-ergy $E_q$ z $E_a$ could exist in some temperature range but it is not clearly evident among the other stages.

As it is evident from Fig. 6 (filled circles), the $E_a$ dependence on the Ga content is strongly nonlinear. Similar dependence was also obtained in Ref. [23] at the study of the epitaxial films of $Ce^{3þ}$ - doped multicomponent $(Gd,Lu)_3(Ga,Al)_5O_{12}$ garnets with different Ga contents. The $E_a$ values obtained in Ref. [25] for the Ce - doped $Gd_3Ga_xAl_{5-x}O_{12}$ crystal with x ¼ 2.83 and for the Ce, Mg - doped crystal with x ¼ 2.69 shown in Fig. 6 by empty squares are also close to the $E_a$ values obtained in the present work and in Ref. [23] for the multicomponent garnets with similar Ga content. However, in case the $E_a$ value is equal to the 5d e CB energy distance and the reduction of the $E_a$ value is caused by the $Ga^{3þ}$ - induced lowering of the CB bottom energy, the dependence of $E_a$ on the Ga content should be linear, similar to those presented in Fig. 6 for the posi-tions of the TSL peaks and the corresponding trap depths $E_t$.

The observed peculiarities of the luminescence thermal quenching and photostimulated defects creation processes in the crystals studied can be explained by the presence of additional energy levels located between the $5d_1$ excited level of $Ce^{3þ}$ and the bottom of the CB. In this case, thermally stimulated electron tran-sitions from the excited $5d_1$ level of $Ce^{3þ}$, resulting in the defects creation, can take place not only to the CB but also to these addi-tional defect levels, and $E_a$ can be considered as the energy differ-ence between the $5d_1$ level and the defect level (d). In Fig. 9, the positions of the $5d_1$ and $5d_2$ excited levels of $Ce^{3þ}$ with respect to the 4f ground state level and the position of the defect level d with respect to the $5d_1$ level of $Ce^{3þ}$ are schematically shown. The approximate position of the CB bottom is presented by dashed line taking into account the data obtained in this work and indicating that (i) in the crystals with x ¼ 1, the $E_a$ value (1.04 eV) corresponds most probably to the energy distance ($E_{dc}$) between the $5d_1$ level and the bottom of the CB or is close to $E_{dc}$; (ii) in the crystal with x ¼ 5, the $5d_1$ level lies inside the CB; (iii) the CB bottom energy decreases linearly with the increasing Ga content. The estimated $E_{dc}$ values are shown in Table 1. The dependences of the band gap energy and the positions of the valence band, conduction band, and the energy levels of $Ce^{3þ}$ on the Ga content in $Gd_3(Ga,Al)_5O_{12}$:Ce have been reported, e.g., in Refs. [6,29,30]. The values of $E_{dc}$ determined in Ref. [29] are presented in Table 1. As it is evident from Table 1, the $E_{dc}$ and $E_a$ values are strongly different, and the $E_{dc}$ values estimated in this work are much larger as compared with those reported in Ref. [29].

As the $E_a$ values obtained for the Ce - and Ce, Mg - doped single crystals and for the Ce - doped epitaxial films of the same (or close) Ga content are very close despite strongly different concentrations of intrinsic defects in the samples studied (for more details, see Refs. [23,25]), the additional defect level d cannot arise from the intrinsic defects. Indeed, the concentration of intrinsic electron traps cannot so strongly (about 50 times) increase with the increasing Ga content from x ¼ 1 to x ¼ 2. Therefore, we suggest that the additional defect levels located below the bottom of the CB can be connected with the $Ga^{3þ}$ ions perturbed by the nearest neighboring $Ce^{3þ}$ ions.

The trapping of electrons, thermally released from the excited $Ce^{3þ}$ levels, by these perturbed $Ga^{3þ}$ ions might result in the

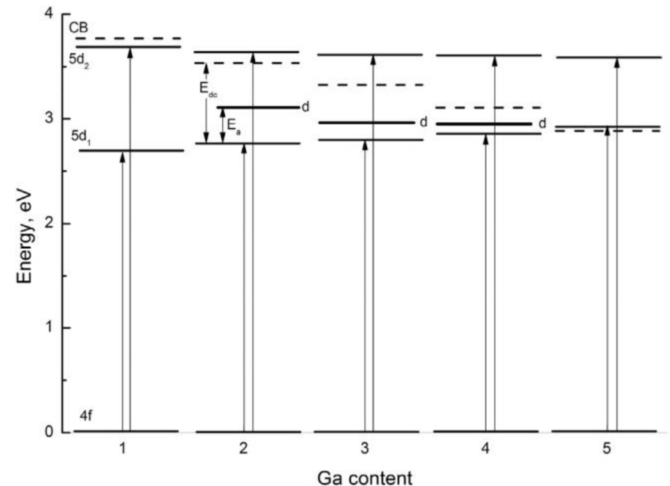


Fig. 9. Positions of the $5d_1$ and $5d_2$ excited levels of $Ce^{3þ}$ and the defect level d (solid lines) and the suggested position of the CB bottom (dashed line) with respect to the 4f ground state level of $Ce^{3þ}$ in $Gd_3Ga_xAl_{5-x}O_{12}$:Ce single crystals with different Ga contents. The 4f - $5d_1$ and 4f - $5d_2$ transitions of $Ce^{3þ}$ ions are shown by arrows. $E_a$ is the energy difference between the $5d_1$ and d levels. $E_{cd}$ is the estimated energy dif-ference between the $5d_1$ level of $Ce^{3þ}$ and the CB bottom.

appearance of the electron $Ga^{2þ}$ centers. The energy levels of Ga are placed around the very bottom of the conduction band [28] so that their participation in creation of electron traps can be expected. Stable $Ga^{2þ}$ centers with visible emission have been intensively studied, e.g., in alkali halide crystals (see, e.g., [31,32]). However, our attempts to detect their luminescence in the irradiated $Gd_3Ga_xAl_{5-x}O_{12}$:Ce crystals were unsuccessful due to the presence of strong $Ce^{3þ}$ - related absorption and emission bands in the considered energy range. The application of EPR for the search of the paramagnetic $Ga^{2þ}$ centers in Gd - containing compounds is not possible as well due to a large nuclear spin of $Gd^{3þ}$. Therefore, the origin of the Ga - related defects will be investigated in more detail in the Gd-free and Ce-doped multicomponent garnets.

## 4. Conclusions

The study of photoluminescence, radioluminescence and TSL characteristics of $Ce^{3þ}$ - doped $Gd_3Ga_xAl_{5-x}O_{12}$ (x ¼ 1, 2, 3, 4, 5) single crystals has revealed their strong dependence on the Ga content. The dependences of the maxima positions of the TSL glow curves and the corresponding trap depths $E_t$ on the Ga content are found to be close to linear. However, the activation energy $E_a$ of the TSL peaks creation under irradiation of the crystals in the 4f e $5d_1$ absorption band of $Ce^{3þ}$ decreases drastically with the increasing Ga content, and this dependence is strongly nonlinear. The conclusion is made that the values of the activation energies for the luminescence thermal quenching ($E_q$) and the TSL peaks creation ($E_a$) are not always equal to the energy distance between the $5d_1$ excited level of $Ce^{3þ}$ and the bottom of the CB. These peculiarities of the Ga - containing multicomponent garnets are suggested to arise from the presence of defect levels located below the bottom of the CB and connected with the $Ga^{3þ}$ ions perturbed by the nearest neighboring $Ce^{3þ}$ ions. This hypothesis as well as the origin and structure of the Ga-related defects in $Gd_3Ga_xAl_{5-x}O_{12}$:Ce need further investigations.

## Acknowledgments

The work was supported by the Institutional Research Funding IUT02-26 of the Estonian Ministry of Education and Research and the project 16-15569S of the Czech Science Foundation.

## References

[1] K. Kamada, T. Endo, K. Tsutumi, T. Yanagida, Y. Fujimoto, A. Fukabori, A. Yoshikawa, J. Pejchal, M. Nikl, Cryst. Growth Des. 11 (2011) 4484e4490.
[2] K. Kamada, T. Yanagida, T. Endo, K. Tsutumi, Y. Usuki, M. Nikl, Y. Fujimoto, A. Fukabori, A. Yoshikawa, J. Cryst. Growth 352 (2012) 88e90.
[3] K. Kamada, T. Yanagida, J. Pejchal, M. Nikl, T. Endo, K. Tsutsumi, Y. Fujimoto, A. Fukabori, A. Yoshikawa, IEEE Trans. Nucl. Sci. 59 (2012) 2112e2115.
[4] M. Nikl, A. Yoshikawa, K. Kamada, K. Nejezchleb, C.R. Stanek, J.A. Mares, K. Blazek, Prog. Cryst. Growth Charact. Mater 59 (2013) 47e72.
[5] M. Tyagi, F. Meng, M. Koschan, S.B. Donnald, H. Rothfuss, C.L. Melcher, J. Phys. D. Appl. Phys. 46 (2013) 475302.
[6] J.M. Ogieglo, A. Katelnikovas, A. Zych, T. Justel, A. Meijerink, C.R. Ronda, J. Phys. Chem. A 117 (2013) 2479e2484.
[7] O. Sakthong, W. Chewpraditkul, Ch. Wanarak, J. Pejchal, K. Kamada, A. Yoshikawa, G.P. Pazzi, M. Nikl, Opt. Mater 36 (2013) 568e571.
[8] T. Yanagida, K. Kamada, Y. Fujimoto, H. Yagi, T. Yanagitani, Opt. Mater 35 (2013) 2480e2485.
[9] W. Drozdowski, K. Brylev, M.E. Witkowski, A.J. Wojtowicz, P. Solarz, K. Kamada, A. Yoshikawa, Opt. Mater 36 (2014) 1665e1669.
[10] K. Brylew, W. Drozdowski, A.J. Wojtowicz, K. Kamada, A. Yoshikawa, J. Lumin. 154 (2014) 452e457.
[11] K. Kamada, S. Kurosawa, P. Prusa, M. Nikl, V.V. Kochurikhin, T. Endo, K. Tsutsumi, H. Sato, Y. Yokota, K. Sugiyama, A. Yoshikawa, Opt. Mater 36 (2014) 1942e1945.
[12] O. Sakthong, W. Chewpraditkul, Ch. Wanarak, K. Kamada, A. Yoshikawa, P. Prusa, M. Nikl, Nucl. Instr. Meth. Phys. Res. A 751 (2014) 1e5.
[13] M. Kitaura, A. Sato, K. Kamada, A. Ohnishi, M. Sasaki, J. Appl. Phys. 115 (2014) 083517.
[14] Y. Wu, F. Meng, Q. Li, M. Koschan, C.L. Melcher, Phys. Rev. Appl. 2 (2014) 044009.
[15] K. Kamada, M. Nikl, S. Kurosawa, A. Beitlerova, A. Nagura, Y. Shoji, J. Pejchal, Y. Ohashi, Y. Yokota, A. Yoshikawa, Opt. Mater 41 (2015) 63e66.
[16] M. Kitaura, A. Sato, K. Kamada, S. Kurosawa, A. Ohnishi, M. Sasaki, K. Hara, Opt. Mater 41 (2015) 45e48.
[17] P. Sibczynski, J. Iwanowska-Hanke, M. Moszynski, L. Swiderski, M. Szawlowski, M. Grodzicka, T. Szczesniak, K. Kamada, A. Yoshikawa, Nucl. Instr. Meth. Phys. Res. A 772 (2015) 112e117.
[18] P. Prusa, M. Kucera, J.A. Mares, Z. Onderisinova, M. Hanus, V. Babin, A. Beitlerova, M. Nikl, Cryst. Growth Des. 15 (2015) 3715e3723.
[19] M.T. Lucchini, V. Babin, P. Bohacek, S. Gundacker, K. Kamada, M. Nikl, A. Petrosyan, A. Yoshikawa, E. Auffray, Nucl. Instr. Meth. Phys. Res. A 816 (2016) 176e183.
[20] A. Yoshikawa, K. Kamada, S. Kurosawa, Y. Shoji, Y. Yokota, V.I. Chani, J. Lumin. 169 (2016) 387e393.
[21] M. Kitaura, K. Kamada, S. Kurosawa, J. Azuma, A. Ohnishi, A. Yamaji, K. Hara, Appl. Phys. Express 9 (2016) 072602.
[22] K. Kamada, Y. Shoji, V.V. Kochurikhin, A. Nagura, S. Okumura, S. Yamamoto, J.Y. Yeom, S. Kurosawa, J. Pejchal, Y. Yokota, Y. Ohashi, M. Nikl, M. Yoshino, A. Yoshikawa, IEEE Trans. Nucl. Sci. 63 (2016) 443e447.
[23] V. Babin, A. Krasnikov, M. Kucera, M. Nikl, S. Zazubovich, Opt. Mater 62 (2016) 465e474.
[24] V. Babin, K. Chernenko, M. Kucera, M. Nikl, S. Zazubovich, J. Lumin 179 (2016) 487e495.
[25] V. Babin, P. Bohacek, L. Grigorjeva, M. Kucera, M. Nikl, S. Zazubovich, A. Zolotarjovs, Opt. Mat. 66 (2017) 48e58.
[26] A. Vedda, M. Nikl, M. Fasoli, E. Mihokova, J. Pechal, M. Dusek, G. Ren, C.R. Stanek, K.J. McClellan, D.D. Byler, Phys. Rev. B 78 (2008) 195123.
[27] R. Chen, S.W.S. McKeever, Theory of Thermoluminescence and Related Phe-nomena, World Scientific Pub. Co., 1997.
[28] M. Fasoli, A. Vedda, M. Nikl, C. Jiang, B.P. Uberuaga, D.A. Anderson, K.J. McClellan, C.R. Stanek, Phys. Rev. B 84 (2011), 081102(R).
[29] P. Dorenbos, J. Lumin. 134 (2013) 310e318.
[30] Y. Wu, J. Luo, M. Nikl, G. Ren, APL Mater. 2 (2014) 012101.
[31] V. Osminin, G. Zavt, S. Zazubovich, A. Niilisk, Bull. Acad. Sci. USSR, Ser. Phys. 38 (1974) 1235e1237.
[32] V. Osminin, S. Zazubovich, Phys. Stat. Sol. B 71 (1975) 435e447.

Institute of Solid State Physics, University of Latvia as the Center of Excellence has received funding from the European Union's Horizon 2020 Framework Programme H2020-WIDESPREAD-01-2016-2017-TeamingPhase2 under grant agreement No. 739508, project CAMART²